Synthesis and Characterization of Monodisperse Core-shell Lanthanide Upconversion Nanoparticles NaYF$_4$: Yb,Tm/SiO$_2$

R. V. Manurung[1], G. Wiranto[1], and I. D. P. Hermida[1]

[1]Research Center for Electronics & Telecommunication – Indonesian Institute of Science Jl. Cisitu No.21/154D, Komplek LIPI Sangkuriang, Bandung, Jawa Barat - 40135, Indonesia

E-mail : rvmanurung@gmail.com

Abstract. Lanthanide up-converting luminescent nanoparticles (UCNPs) are exciting and promising materials for optical bioimaging, biosensor and theranostic due to their unique and advantageous optical and chemical properties. The UCNPs absorb low energy near-infrared (NIR) light and emit high-energy shorter wavelength photons (visible light). Their unique features allow them to overcome various problems associated with conventional imaging probes such as photostability, lack of toxicity, and to provide versatility for creating nanoplatforms with both imaging and therapeutic modalities. This paper reports synthesis and characterization of core-shell structured of NaYF$_4$:Yb,Tm/SiO$_2$ microspheres. The synthesis of lanthanide upconversion nanoparticles NaYF$_4$:Yb,Tm was prepared by thermal decomposition process which involves dissolving organic precursors in high-boiling-point solvents oleic acid (OA) and octadecene (ODE). After that, the NaYF$_4$:Yb,Tm phosphors was coated by silica via reverse microemulsion process to obtain core-shell structured NaYF$_4$:Yb,Tm/SiO$_2$. Scanning electron microscopy, transmission electron microscopy, specific area electron diffraction, and photoluminescence were applied to characterize these samples. The obtained core-shell structured NaYF$_4$:Yb,Tm/SiO$_2$ phosphors exhibit a perfect cubic morphology with narrow size distribution and smooth surface. Upon IR excitation at 980 nm, the NaYF$_4$:Yb,Tm/SiO$_2$ samples exhibit whitish blue upconversion (UC) luminescence, respectively. These phosphors show potential applications in the displaying on biological fields and biosensing.

Keywords. Core-shell, lanthanide, photoluminescence, and upconversion.

1. Introduction

Organic dyes and fluorescent proteins have been used for fluorescent probes in biological detections including bioimaging and biosensing in last decades. It is well known that organic fluorescent dyes have several advantages such as small size, excellent biocompatibility, easy surface modifications for covalent conjugations, and relatively high fluorescent intensity [1]. However, some drawbacks have been found such as short detection times due to high photobleaching efficiency and chemical degradation [2]. Also, organic dyes have narrow absorption and broad emission spectra with long tailing which limits their detection [1–2]. Semiconductor quantum dot (QD) has advantages compared to conventional organic dyes such as size-tunable emission, bright photoluminescence, good photostability, broad ultraviolet (UV) excitation and narrow emission have emerged as alternative and promising fluorescent labels agent [3]. However, QD has several drawbacks such as cytotoxicity issue,

and chemical instability[4] have limited application for long-term usage. Moreover, UV or short wavelength excitation usually required by traditional biolabels such as organic dyes, fluorescent proteins, and QDs. The short wavelength may result in severe limitations such as low light-penetration depth, possible damage or even death of biomolecules caused by long-term irradiation, and low signal-to-noise ratio due to significant autofluorescence (background) from biological samples in the UV short wavelength regions.

Nowadays, non-linear optical processes phenomena known as upconversion (UC) where the conversion of near-infrared radiations into visible light by combining two or more low energy photons to generate a single high-energy photon by an anti-Stokes process. The applications of upconversion nanoparticles (UCNPs) have become very prominent in bioimaging and biosensor field. In particular, UCNPs serve as an alternative and excellent substitute for traditional fluorescent labels. In contrast to conventional luminescent probes, UCNPs exhibit a great photostability, sharp multi-peak line emission, and continuous emission capability. Furthermore, light scattering by biological tissues is substantially reduced with near-infrared (NIR) excitation. By absorb NIR excitation result in the reduction in light scattering, and it implies in depth of penetration in tissue much more significant than that obtained under ultraviolet or visible excitation [5]. UCNPs typically comprises three key components: a host matrix, a sensitizer (absorber) and an activator [6]. The host matrix is one of the essential elements of UCNPs due to their essential and unique UC optical properties, including luminescence efficiency and emission profile. The sensitizer can be efficiently excited from specific light source and then transfers the energy to the activator where radiation can be emitted. Thus, the activator is the luminescence center in UCNPs, and the sensitizer enhances the UC luminescence efficiency. The dopants, sensitizer, and activator are added to the host lattice in relatively low concentrations (~20 mol% for the sensitizer and ~2 mol% for the activator). The trivalent Yb^{3+} ion, having a straightforward energy level scheme, therefore it is suitable as a sensitizer. Er^{3+}, $Tm^{3+,}$ and Ho^{3+} ions have energy levels in the form of a ladder and hence are most frequently used as UC activators. Among the available types of UC host materials, fluorides have proven to be ideal host candidates for UC because of their very low phonon energies and high chemical stability.

In this paper, we report the synthesis of UCNPs of $NaYF_4$:Yb,Tm in oleic acid (OA) and octadecene (OD) by thermal decomposition method and followed by a SiO_2 coating by using microemulsion for water dispersibility. Transmission electron microscopy, scanning electron microscopy, specific area electron diffraction, and photoluminescence emission were applied to characterize these samples.

2. Materials and methods

2.1. Synthesis of NaYF₄:Yb,Tm nanocrystals
All the chemicals used in this work were purchased from Sigma-Aldrich without further purification. $NaYF_4$:25%Yb, 0.3%Tm nanocrystals were synthesized as follows [7]: 0.75 mmol YCl_3 (Yttrium trichloride, 99.99 %), 0.25 mmol $YbCl_3$ (ytterbium(III)chloride, 99.99 %) and 0.003 mmol $TmCl_3$ (thulium(III)chloride) were mixed with 6 mL oleic acid (OA) and 15 mL octadecene (ODE) in a 50 mL flask. The solution was heated to 160 °C to form a homogeneous solution and then cooled down to room temperature. Then, 10 mL methanol solution containing NaOH (2.5 mmol) and NH_4F (4 mmol) was slowly added to the mini schlenk line flask then stirred for 30 min. The solution was slowly heated to remove methanol, degassed at 100 °C for 10 min, and followed by heating at 300 °C and maintained for 1 h under inert gas protection. After the solution was cooled naturally, nanocrystals were precipitated from the solution with ethanol and washed with ethanol/water (1:1 v/v) for three times.

2.2. Synthesis of the SiO₂ shell on the NaYF₄:Yb,Tm nanoparticles
The hydrophobic $NaYF_4$:Yb,Tm nanocrystals, in hexane, surfactants, and ammonia were added to form a water-in-oil reverse microemulsion. A relatively high nanocrystal concentration was used, and

the emulsion was sonicated to ensure that all the nanocrystals were encapsulated in a microemulsion pool. Firstly we prepared a mixture of 0.1 mL of CO-520 (IGEPAL), 6 mL of hexane, and 4 mL of 10 mM NaYF$_4$:Yb,Tm nanoparticles in hexane solution. The solution was stirred for 10 min; 0.4 mL of CO-520 and then add 0.08 mL of 30 wt% ammonia followed by sealing the container. The container was then sonicated for 20 min until a transparent emulsion was formed. Then, 0.04 mL of TEOS was added to the solution. The solution was then stirred for 48 h at 600 rpm. NaYF$_4$:Yb,Tm/SiO$_2$ core/shell nanoparticles were precipitated by adding acetone and washed twice with ethanol/water (1:1 v/v), and then re-dispersed in water.

2.3. Characterization
SEM and TEM images of the nanocrystals were obtained using a FESEM 6700F, JEOL, Japan and FEI Tecnai G2 20 S-Twin transmission electron microscope equipped with energy dispersive spectroscopy (EDS) and selective area diffraction (SAD), respectively. Upconversion fluorescence spectra were obtained on a Maya2000 Pro spectrometer from Ocean Optics with an external 980 nm laser (5 W, continuous wave Shanghai Dream laser) as the excitation source.

3. Results and discussion

3.1. Morphology and structure of the nanocrystals
Figure 1.a exhibited the morphology of NaYF$_4$:Yb,Tm under SEM investigation while Figure 1.b showed the TEM images of the as-prepared core NaYF$_4$:Yb,Tm and the core-shell NaYF$_4$:Yb,Tm/SiO$_2$ nanoparticles. Under TEM investigation, UCNPs with spherical morphology were observed, which indicated that the adsorption of the hydrophobic capping ligand of oleic acid on the crystal surface prevented the further aggregation of NaYF$_4$ toward macroscopic crystals, leading to the formation of the nanocrystal. UCNPs also possessed narrow size distribution with an average diameter of 10 nm. High magnification TEM image on inset indicated that the core NaYF$_4$:Yb,Tm were single crystal, with an interplanar distance of 0.3 nm (Figure 1.b). The problem of thermal decomposition is that it typically produces nanocrystals with hydrophobic surfaces. The ideal luminescence nanoparticles used for biology should meet several requirements, such as being homogeneously dispersed and colloidally stable in aqueous solvents, maintaining a high quantum yield and showing high specific binding to biological components. The insolubility of such nanocrystals in aqueous solution thus greatly limits their bio-applications and silica coating as one of the solutions to overcome the problem. Silica layer on the core UCNPs surface has been succeeding to growth by reverse microemulsion as a common technique of SiO$_2$ coating along with Stober method [8]. The dense amorphous SiO$_2$ shell thickness can be tuned by changing the concentration of tetraethyl orthosilicate (TEOS). However, coating single nanoparticles with uniform thin shells are very challenging [9–10]. The inset of Figure 1.c exhibit ± 7 nm thickness of SiO$_2$ shell on the surface of NaYF$_4$:Yb,Tm.
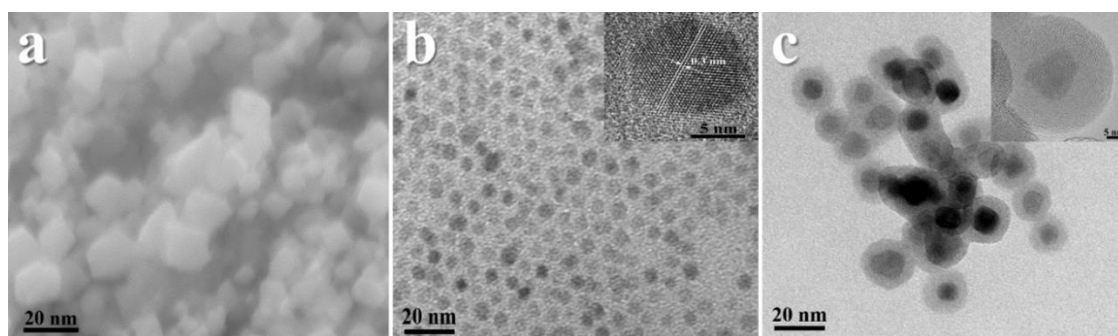
Figure 1. (a) SEM, and TEM images of (b) the core NaYF$_4$:Yb,Tm (c) the core-shell NaYF$_4$:Yb,Tm/SiO$_2$ nanoparticles. The inset in b, and c refer to high magnification TEM images of the core and core-shell, respectively.

3.2. Upconversion Fluorescence and elemental properties of upconversion nanoparticles

Fluorescence spectra of transparent colloidal solutions of NaYF$_4$:Yb,Tm nanospheres in hexane is shown in Figure 2.a. The emission peaks of NaYF$_4$:Yb,Tm nanospheres has been observed at 360, 450, 478, 649, 679, 700 and 800 nm were due to the electrons transitions from the energy levels $^1D_2 \rightarrow$ $^3H_6$; $^1D_2 \rightarrow$ $^3F_4$; $^1G_4 \rightarrow$ $^3H_6$; $^1G_4 \rightarrow$ $^3F_4$; $^3H_5 \rightarrow$ $^3H_6$, $^3F_2 \rightarrow$ $^3H_6$ and $^3H_4 \rightarrow$ $^3H_6$ [11]. The inset of figure 2(a) exhibited an optical photograph of quartz cuvette showing blue luminescence from core NaYF$_4$:Yb,Tm nanocrystals and it is showed that the color obtained from highly radiative relaxation from the electron which is populated on the blue region (478 nm). The luminescence and radiant transition result of our core NaYF$_4$:Yb,Tm nanocrystals indicate the similar result with previous publication reported by Sudheendra *et al* [12]. However, our radiant transition and fluorescence spectra exhibit more additional peaks compare to the results reported by Sudheendra *et al* [12]. Moreover, the core of UCNPs displayed higher optical absorption around 977 nm which indicate a match with excitation wavelength as shown in Figure 2.b due to utilizing ion pairs (sensitizer/activator) of Yb^{3+}/Tm^{3+} for enhanced excitation at ~975 nm. The result indicates Yb^{3+} works perfectly as a sensitizer, as it has a sufficiently large absorption cross-section in the NIR region at ~975 nm [13]. The energy dispersive spectroscopy indicated their chemical symbol identifies different elemental peaks. The EDS result confirmed the presence of Yb and Tm in the upconversion nanoparticles, and the amount of Y, Yb, and Tm was quantified using this technique. Figure 2(d) shows the selected area diffraction (SAD) pattern of the NaYF$_4$:Yb,Tm nanocrystals. The positions of the polycrystalline diffraction ring corresponding to the (111), (200), (220), (311), (222), (400), (331) and (420) planes. These identified planes agreed with the single-phase cubic or alpha (α) NaYF$_4$ crystals (JCPDS: 06-0342), and no peaks of impurities were detected [11, 12]. The result shows that thermal decomposition method is an appropriate method for preparing doped NaYF$_4$ nanocrystals with a purely cubic phase. The SAED result also suggests that NaYF$_4$:Yb,Tm successfully crystallize on the surface amorphous SiO$_2$ as an outer coating layer. No other phase related with the doped Yb^{3+} and Tm^{3+} can be observed, indicating the high purity of the sample.
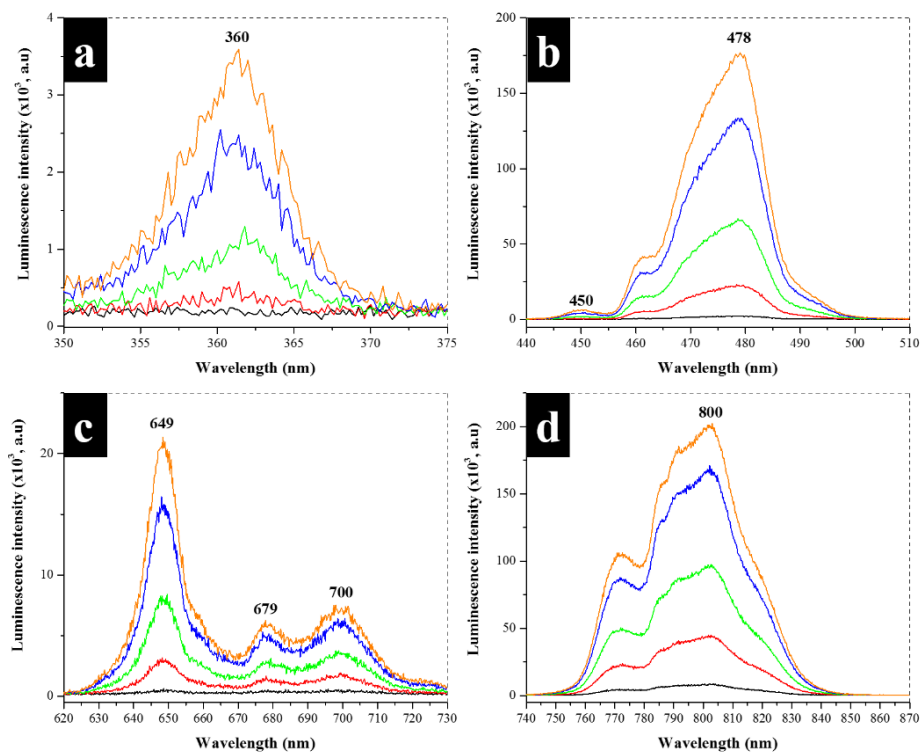
Figure 3 showed the luminescence spectra of NaYF$_4$:Yb,Tm at a various excitation power of 980 nm laser source start from 1 W to 5 W. Each of signature peak of NaYF$_4$:Yb,Tm indicated upconversion process was observed at (360, 450, 478, 649, 679, 700 and 800) nm. These peaks were associated to the electrons transitions from the energy levels $^1D_2 \rightarrow$ $^3H_6$; $^1D_2 \rightarrow$ $^3F_4$; $^1G_4 \rightarrow$ $^3H_6$; $^1G_4 \rightarrow$ $^3F_4$; $^3H_5 \rightarrow$ $^3H_6$, $^3F_2 \rightarrow$ $^3H_6$ and $^3H_4 \rightarrow$ $^3H_6$ [11] and plot as shown in Figure 3 (a to d). The result indicates either core and core-shell of NaYF$_4$:Yb,Tm/SiO$_2$ has consistent respond on each of the signature peaks of luminescence spectra to different excitation power. The result also provides understanding that the more incoming photon from 980 lasers by increasing power excitation. The more electron transition transfer within the electronic state of lanthanide trivalent (Yb^{3+} and Tm^{3+}) produced upconversion luminescence as mentioned as well by Sudheendra *et al* [12] and Chen *et al* [13]. The up-conversion photoluminescence intensity (I$_{pl}$) has a dependence on the power (P) of the excitation light given by [13]

$$I_{pl} = KP^n$$
(1)

where 'n' is an integer that determines the number of photons utilized in the photoluminescence process, and K is a material-related coefficient.
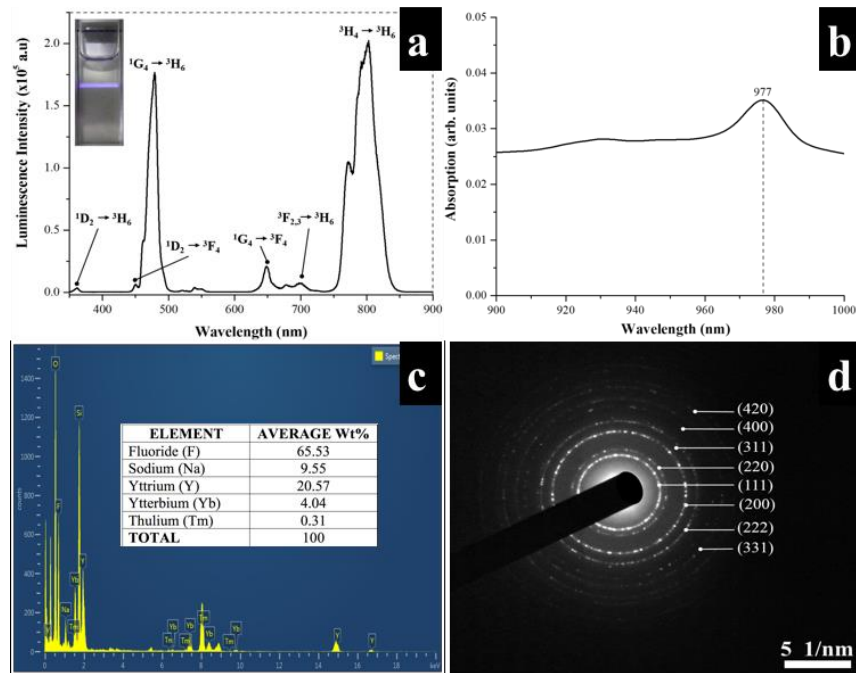
Figure 2. (a) The luminescence spectra of NaYF$_4$:Yb,Tm emission in hexane, under excitation power 5 W of 980 nm, (b) absorption spectra, (c) energy dispersive spectra (EDS), and (d) selected area diffraction (SAD). Their chemical symbols identify the elemental peaks in the EDS (c), and diffraction rings are distinguished (by the arrows and Miller indices) according to JCPDS No. 06-0342 (d).

Figure 3. The luminescence spectra of the (a) 360 (b) 450, 478 (c) 649, 679, 700 and (d) 800 nm peak emission of NaYF$_4$:Yb, Tm in hexane, under different excitation power 1-5 W of 980 nm.

4. Conclusions

A monodisperse and purely cubic phase of $NaYF_4$:Yb,Tm nanocrystals were prepared with oleic acid and octadecene as a chelating agent and stabilizer have obtained by thermal decomposition method. The nanocrystals have average diameter ±10 nm with lattice spacing 0.3 nm. SiO_2 coating has been succeeding by reverse microemulsion to increase solubility, and the thickness was around 7 nm and can be adjusted by controlling the concentration of TEOS during hydrolysis. Under 980-nm excitation, the core-shell $NaYF_4$:Yb,Tm/SiO_2 upconversion nanoparticles emit strong upconversion fluorescence. The further application of UCNPs $NaYF_4$:Yb,Tm has open new opportunities in fields such as bioimaging, biosensor and photodynamic therapy.

References

[1]   Shen J *et al* 2008 Luminescent rare earth nanomaterials for bioprobe applications *Dalton Trans.* **42** pp 5687–5697

[2]   Smith A M *et al* 2004 Quantum dot nanocrystals for in vivo molecular and cellular imaging *Photochem Photobiol.* **80** pp 377–385

[3]   Chan W C W and Nie S M 1998 Quantum dot bioconjugates for ultrasensitive nonisotopic detection *Science* **281** pp 2016–2018

[4]   Chang E *et al* 2006 Evaluation of Quantum Dot Cytotoxicity Based on Intracellular Uptake *Small* **2** pp 1412–1417

[5]   Zhang Y *et al* 2014 *Chem. Soc.* **136** pp 4893–4896

[6]   Wang F and Liu X G 2009 Recent advances in the chemistry of lanthanide-doped upconversion nanocrystals *Chem. Soc. Rev.* **38** pp 976–989

[7]   Manurung R V *et al* 2016 A plasmon-tuned 'gold sandwich'for metal enhanced fluorescence in silica coated $NaYF_4$: Yb, Er upconversion nanoparticles *RSC Adv* **6** pp 87088–87095

[8]   Zhang H *et al* 2011 Highly spectral dependent enhancement of upconversion emission with sputtered gold island films *Chem. Commun.* **47** pp 979–981

[9]   Eichailbum M and Rademann K 2009 Plasmonic Enhancement or Energy Transfer On the Luminescence of Gold-, Silver-, and Lanthanide-Doped Silicate Glasses and Its Potential for Light-Emitting Devices *Adv. Funct. Mater.* **19** pp 2045–2052

[10]   Verhagen E, Kuipers L and Polman A 2009 Field enhancement in metallic subwavelength aperture arrays probed by erbium upconversion luminescence *Opt. Express* **17** pp 14586–14598

[11]   Yin A X *et al* 2010 Colloidal synthesis and blue based multicolor upconversion emissions of size and composition controlled monodisperse hexagonal NaYF 4: Yb, Tm nanocrystals *Nanoscale* **2** pp 953–959

[12]   Sudheendra L *et al* 2011 *Chem. Mater.* **23** pp 2987–2993

[13]   Chen G *et al* 2014 *Chem. Rev.* **114** 5161–5214